



SUPPLEMENTARY MATERIAL TO

**Zinc oxide nanoparticles prepared by thermal decomposition of
zinc benzenepolycarboxylato precursors:
Photoluminescent, photocatalytic and antimicrobial properties**

LIDIJA RADOVANOVIĆ^{1*}, JELENA D. ZDRAVKOVIĆ¹, BOJANA SIMOVIĆ²,
ŽELJKO RADOVANOVIĆ¹, KATARINA MIHAJLOVSKI³,
MIROSLAV D. DRAMIĆANIN⁴ and JELENA ROGAN³

¹Innovation Centre of Faculty of Technology and Metallurgy, University of Belgrade, Karnegijeva 4, Belgrade, Serbia, ²Institute for Multidisciplinary Research, University of Belgrade, Kneza Višeslava 1, Belgrade, Serbia, ³Faculty of Technology and Metallurgy, University of Belgrade, Karnegijeva 4, Belgrade, Serbia and ⁴Vinča Institute of Nuclear Sciences, University of Belgrade, P. O. Box 522, Belgrade, Serbia

J. Serb. Chem. Soc. 85 (11) (2020) 1475–1488

EXPERIMENTAL

Solid-state kinetics under non-isothermal conditions

The general equation (Eq. (1)) was used to describe the kinetics of thermally induced reactions in the solid state:¹

$$\frac{d\alpha}{d\tau} = A \exp\left(-\frac{E_a}{RT}\right) f(\alpha) \quad (1)$$

where E_a is the apparent activation energy, A is the pre-exponential factor, and $f(\alpha)$ is an algebraic expression of the kinetic model as a function of conversion degree, α . The value of α , at any temperature and for all heating rates was determined as

$$\alpha = \frac{m_i - m}{m_i - m_f} \quad (2)$$

where m is the mass of a sample at a certain temperature, while m_i and m_f are the initial and final masses, respectively. In DTG data, α represents the ratio of the partial peak surface area for a given temperature in relation to the total peak surface area.

Under non-isothermal conditions, for measurements at constant heating rates, Eq. (1) is usually converted to:

$$\beta \frac{d\alpha}{d\tau} = A \exp\left(-\frac{E_a}{RT}\right) f(\alpha) \quad (3)$$

where β is the heating rate, $\beta = dT/d\tau$. The integral form (Eq. (4)) of the reaction can be obtained by integrating Eq. (3) as:

*Corresponding author E-mail: radovanovic@tmf.bg.ac.rs

$$g(\alpha) = \int_0^{\alpha} \frac{d\alpha}{f(\alpha)} = \frac{AE_a}{R\beta} p(x) \quad (4)$$

where $p(x)$ is the temperature integral for $x = E_a/RT$, which does not have an analytical solution.²

The non-isothermal kinetic analysis of complexes **1–4** was performed under four heating rates (15, 20, 25 and 30 °C min⁻¹) using the Kissinger method:³

$$\ln \frac{\beta}{T^2} = \ln \frac{AR}{E_a} - \frac{E_a}{RT} \quad (5)$$

where T is the temperature corresponding to the maximum of the DTG peak.

The thermodynamic activation parameters, change of activation entropy (ΔS^\ddagger), activation enthalpy (ΔH^\ddagger) and Gibbs free energy of activation (ΔG^\ddagger) were calculated for all degradation steps,^{4,5} using Eqs. (6)–(8):

$$\Delta S^\ddagger = R \left[\ln \frac{Ah}{k_B T} \right] \quad (6)$$

$$E_a \approx \Delta H^\ddagger - RT \quad (7)$$

$$\Delta G^\ddagger = \Delta H^\ddagger - T \Delta S^\ddagger \quad (8)$$

where h and k_B are the Planck's and the Boltzmann's constants, respectively.

RESULTS AND DISCUSSION

TABLE S-I. Thermogravimetric results for precursors **1–4**

Precursor	Stage	TG range, °C	DTG peak temperature, °C	Mass loss, % (Calc., %)	Fragment loss	Residue
1	1	30–386	365	36.9 (34.2)	-C ₅ H ₅ N ₂ + CO ₂	
	2	386–465	432	26.7 (26.5)	-C ₅ H ₄ N + CO	
	3	465–548	511	19.0 (17.4)	-C ₆ H ₄	ZnO
2	1	30–411	402	30.5 (30.5)	-C ₅ H ₄ N + CO ₂	
	2	411–486	441	30.1 (30.2)	-C ₅ H ₄ N ₂ + CO	
	3	486–560	510	18.7 (18.9)	-C ₆ H ₄	ZnO
3	1	30–175	159	4.33 (4.30)	H ₂ O	
	2	175–348	310	17.0 (17.2)	CO ₂ + CO	
	3	348–440	391	36.8 (36.8)	-C ₅ H ₄ N + -C ₆ H ₄	
	4	440–504	491, 502	24.7 (22.0)	-C ₅ H ₄ N ₂	ZnO
4	1	30–461	420	53.5 (53.4)	2C ₁₀ H ₉ N ₃ + CO ₂	
	2	461–540	509	21.0 (20.1)	-C ₆ H ₂ + CO + CO ₂	2ZnO

TABLE S-II. Thermodynamic and kinetic parameters of the thermal degradation of 1–4

Precursor	Stage	$E_a / \text{kJ mol}^{-1}$	$\ln(A / \text{min}^{-1})$	$\Delta H^\ddagger / \text{kJ mol}^{-1}$	$\Delta S^\ddagger / \text{J mol}^{-1} \text{K}^{-1}$	$\Delta G^\ddagger / \text{kJ mol}^{-1}$
1	1	235.7 ± 1.9	44.7 ± 10.6	230.4	86.2	175.4
	2	163.9 ± 2.4	27.8 ± 10.3	158.0	-54.6	196.5
	3	75.8 ± 2.9	10.4 ± 9.6	69.3	-200.3	226.4
2⁶	1	284.1 ± 9.0	51.0 ± 12.0	278.5	138.6	191.1
	2	254.9 ± 10.6	43.1 ± 12.8	248.9	72.2	203.3
	3	105.6 ± 6.5	15.4 ± 10.5	99.1	-160.2	231.1
3	1	100.6 ± 1.3	28.3 ± 9.8	97.0	-46.5	117.1
	2	136.6 ± 2.2	28.1 ± 10.2	131.8	-50.8	161.4
	3	294.2 ± 13.4	52.7 ± 12.9	288.7	152.9	187.1
	4	196.5 ± 6.7	29.9 ± 11.1	190.1	-37.8	219.4
4	1	296.5 ± 11.4	51.8 ± 14.2	290.7	145.0	190.2
	2	68.1 ± 0.6	9.1 ± 8.1	61.5	-211.1	226.7

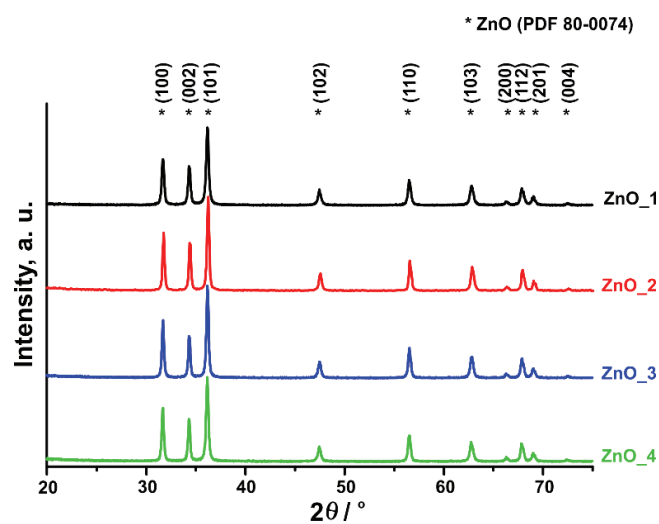


Fig. S-1. XRPD patterns of ZnO_1–ZnO_4.
Diffraction peaks are indexed according to PDF 80-0074.

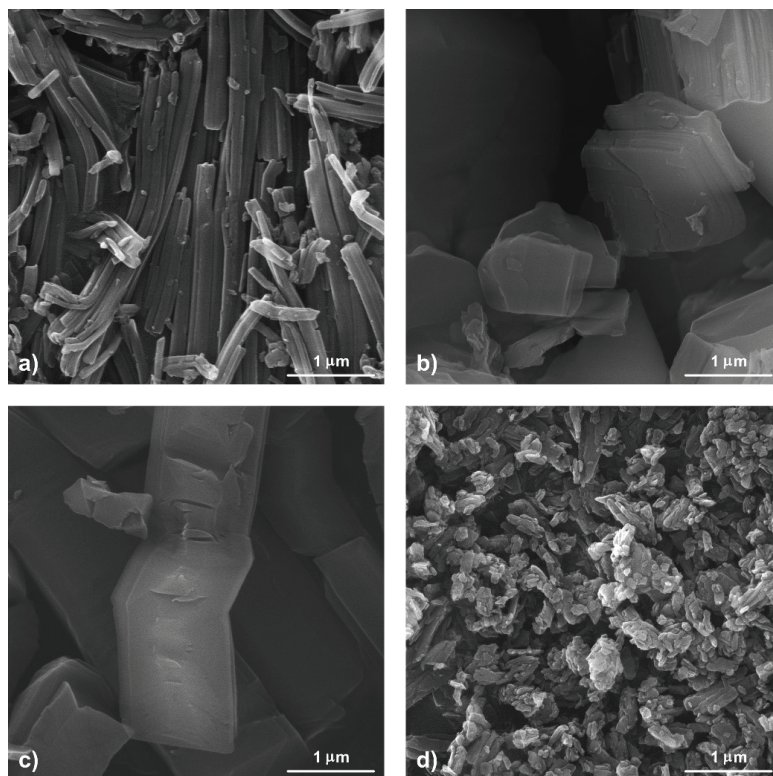


Fig. S-2. FESEM images of precursors **1** (a), **2** (b), **3** (c) and **4** (d).

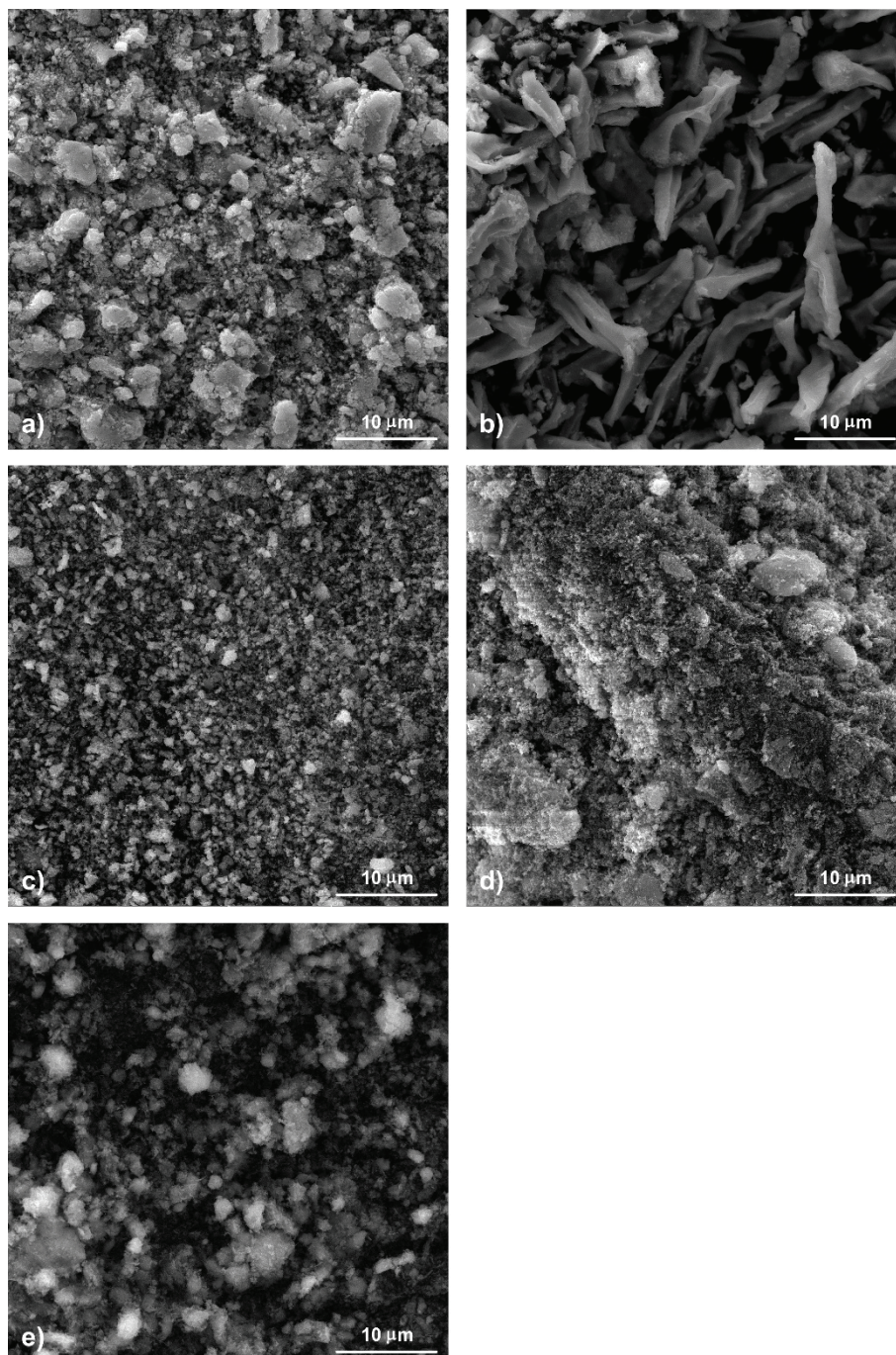


Fig. S-3. FESEM images of agglomerated ZnO_1 (a), ZnO_2 (b), ZnO_3 (c), ZnO_4 (d) and ZnO_com (e) at magnification of 5000 \times .

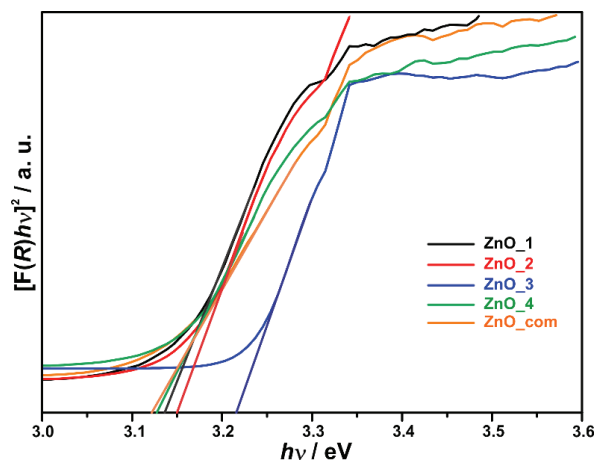


Fig. S-4. Plot of $(F(R)h\nu)^2$ as a function of photon energy for ZnO_1–ZnO_4 and ZnO_com.

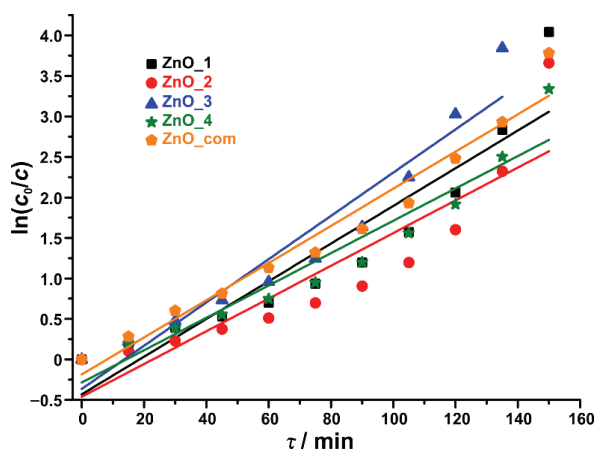


Fig. S-5. Linear plots of pseudo-first order kinetic model of RO16 degradation on the investigated ZnO powders.

REFERENCES

1. S. Vyazovkin, *Thermochim. Acta* **355** (2000) 155 ([https://doi.org/10.1016/S0040-6031\(00\)00445-7](https://doi.org/10.1016/S0040-6031(00)00445-7))
2. S. Vyazovkin, K. Chrissafis, M. L. Di Lorenzo, N. Koga, M. Pijolat, B. Roduit, N. Sbirrazzuoli, J. J. Suñol, *Thermochim. Acta* **590** (2014) 1 (<https://doi.org/10.1016/j.tca.2014.05.036>)
3. H. E. Kissinger, *Anal. Chem.* **29** (1957) 1702 (<https://doi.org/10.1021/ac60131a045>)
4. H. J. Eyring, *J. Chem. Phys.* **3** (1935) 107 (<https://doi.org/10.1021/cr60056a006>)
5. M. G. Evans, M. Polanyi, *Trans. Faraday Soc.* **31** (1935) 875 (<https://doi.org/10.1039/TF9353100875>)
6. J. D. Zdravković, L. Radovanović, D. Poleti, J. Rogan, P. Vulić, Ž. Radovanović, D. M. Minić, *Solid State Sci.* **80** (2018) 123 (<https://doi.org/10.1016/j.solidstatesciences.2018.04.013>).